Microchim Acta (2016) 183:73–81
DOI 10.1007/s00604-015-1590-9

ORIGINAL PAPER

Microbial glucose biosensors based on glassy carbon paste electrodes modified with *Gluconobacter Oxydans* and graphene oxide or graphene-platinum hybrid nanoparticles

Sema Aslan[1] · **Ülkü Anik**[1]

Received: 20 May 2015 / Accepted: 1 August 2015 / Published online: 13 August 2015

Abstract We have performed a study on the performance of two microbial glucose sensors based on immobilized *Gluconobacter oxydans* (*G. oxydans*). The first one was prepared by modifying a glassy carbon paste electrode (GCPE) containing the microbial cells with graphene oxide (GO), the other one by modifying it with graphene-platinum hybrid nanoparticles (graphene-Pt NPs). The electrode was characterized by following the voltammetric signals of the oxidation of hexacyanoferrate(II) to hexacyanoferrate(III) via the oxidative enzymes contained in *G. oxydans* which convert glucose to gluconic acid. Optimizations were conducted with a conventional GCPE containing *G. oxydans*. After material optimization, the biosensors were applied to the determination of glucose. The linear and analytical ranges for GO based biosensor range from 1 to 75 μM (linear) and 1 to 100 μM (analytical), respectively, with a limit of detection (LOD) of (3 s/m) 1.06 μM (at an S/m of 3). On the other hand, the graphene-Pt hybrid nanoparticle based biosensor showed two linear ranges (from 0.3 to 1 μM and from 1 to 10 μM), a full analytical range from 1 to 50 μM, and an LOD of 0.015 μM. The graphene-Pt hybrid NP based sensors performs better and was applied to the determination of glucose in synthetically prepared plasma samples where it gave recoveries as 101.8 and 104.37 % for two different concentrations. Selectivity studies concerning fructose, galactose, L-ascorbic acid and dopamine were also conducted.

Keywords Graphene oxide · Graphene-platinum hybrid nanoparticles · *Gluconobacter oxydans* · Nanomaterials · Microbial biosensor

Introduction

Nanomaterials like carbon nanotubes (CNTs) have been often incorporated to electrochemical biosensors. These nanomaterials have fascinating electrical conductivity and catalytic effects [1–3]. Since its discovery in 2004, another carbon based nanomaterial, viz. graphene, has become an intensively studied material due to its excellent conductivity and electrocatalytic activity. It has been shown that graphene's sp^2 forms of two dimensional sheets are responsible for fast electron transfer at the edges. Because of this, graphene and another form of graphene, graphene oxide (GO) have been extensively used for electroanalytical purposes [4–9]. For example, Pumera reported that graphene shows many advantages for electrochemical applications when compared to graphite or CNTs [4]. Wang et al. fabricated a graphene-modified dopamine sensor and reported that this electrode showed better performance than multiwalled carbon nanotube-modified electrode [5]. The immobilization of the probe DNA on the surface of electrode was largely improved by Bo et al. by using oxidized graphene [6]. Also Shan et al. reported a glucose oxidase (GOx) based biosensor and pointed to the good electrocatalysis toward oxygen and H_2O_2 in the presence of graphene [7]. Zhou et al. also mentioned about the single sheet structure of graphene that shows favorable electrochemical activity [8].

On the other hand, decorating carbon based nanomaterials like CNTs with noble metal NPs which results as effective

Electronic supplementary material The online version of this article (doi:10.1007/s00604-015-1590-9) contains supplementary material, which is available to authorized users.

✉ Ülkü Anik
ulkuanik@yahoo.com; ulkuanik@gmail.com

[1] Faculty of Science, Chemistry Department, Mugla Sitki Kocman University, 48000 Kötekli, Mugla, Turkey

nanocomposites are not new [10, 11]. These nanocomposites surely used in many areas as catalysts. However CNT production is complicated and has high cost compared to graphene production which simply includes the chemical conversion of inexpensive graphite. As metallic Np combined with graphene, highly dispersed platinum (Pt)-NPs onto both sides of graphene sheets which have larger surface areas, should be resulted with some significant benefits especially in electrochemistry and nanotechnology research areas. [11–14].

Recently our group demonstrated that graphene-Pt hybrid NPs shows better electrocatalytic activity compared to GO in electrochemical genosensors and in biofuel cells. This electrocatalytic enhancement was explained by the combined electrocatalytical activity of Pt with important properties of graphene [15, 16]. Considering these studies, for graphene-Pt hybrid NPs preparation, we used the method suggested by Xu et al. [11]. In this method, ethylene glycol (EG)-water mixture has been used as the reducing reagent in the presence of metallic salts which act as catalysts. Xu et al. manage to demonstrate that, without any metallic salt, no reduction was observed onto GO sheets. When suitable metallic salts like Pt, Pd and Au were added, the deoxygenation of GO together with accumulation of these metallic NPs onto graphene sheets were achieved. Besides, it is also shown that these metallic salts prevent restack of these sheets during the chemical reduction process [11]

In this work, we examined the electrochemical performance of graphene-Pt hybrid NP and GO for microbial biosensor. For the construction of microbial biosensor, *G. oxydans* together with graphene were introduced into composite glassy carbon paste electrode (GCPE).

Gluconobacter sp. has ability to oxidize a wide range of organic compounds with a low growth yield. For this reason, they have been extensively used in biotechnological areas, like biosensors [17]. Because of their interfacial electrochemical properties like direct electron transfer and direct bioelectrocatalysis, Gluconobacter enzymes have also been used in biofuel cells [18].

After the characterization of graphene based nanomaterials, optimization studies were carried out with *G.oxydans*/GCPE biosensor. Then, graphene based NPs were introduced into electrode structure and analytical characteristics were examined. Based on the obtained analytical characteristics, the electrochemical performances of graphene-Pt hybrid NP/ *G.oxydans*/GCPE and GO/ *G.oxydans*/GCPE microbial biosensors were also compared.

Experimental

Materials

HCl, NaCl, H_2SO_4, H_2O_2, $NaNO_3$, $CaCl_2$, KCl, urea, $MgCl_2$, Tris–HCl and $KMnO_4$ were purchased from Merck (www.merckmillipore.com, Germany). H_2PtCl_6, EG, $HAuCl_4.3H_2O$, sodium citrate, D-Fructose, D-Galactose (bioreagent grade), KBr, L-Ascorbic acid, dopamine, bovine serum albumin and immunoglobulin G were purchased from Sigma-Aldrich (www.sigmaaldrich.com, USA). KH_2PO_4 was used to prepare phosphate buffer (PB), for pH adjustment 1.0 M $NaOH_{(aq)}$ was used and both of these chemicals were purchased from Merck (www.merckmillipore.com, Germany). Yeast extract granulated and D (+) Glucose monohydrate (www.merckmillipore.com, Germany) were used at bacterial growth medium. $K_3Fe(CN)_6$ was used as probe for all electrochemical measurements and purchased from Sigma (www.sigmaaldrich.com, USA). Glassy carbon, spherical powder (2.0-12 μm) (www.sigmaaldrich.com, USA) and mineral oil were used at preparation of electrodes. All of other chemicals were of analytical grade. All experiments were performed at room temperature.

Instruments

μ-AUTOLAB TYPE III electrochemical analyzer was equipped with GPES/FRA and used for electrochemical measurements (www.metrohm-autolab.com). A standard three-electrode cell contained a platinum wire as auxiliary electrode, an Ag|AgCl (Ag/AgCl/KCl (1.0 M)) (filled with 1.0 M KCl, METROHM (www.metrohm.com)) as reference electrode and *G.oxydans*/GCPE or *G.oxydans*/GO/GCPE or *G. oxydans*/ graphene-Pt hybrid NP/GCPE was used as working electrode. The electrodes were inserted into a conventional electrochemical cell. Sonication was performed with Bandelin Sonorex sonicator. Scanning electron microscopy (SEM) measurements were performed at JSM-7600 F FEG SEM at 15.0 kV. Also JEOL-JEM 2100 F used for transmission electron microscopy (TEM). BIOSAN environmental shaker incubator ES-20 was used as rotary shaker incubator (www.biosan.com), SIGMA 3–16 PK was used at centrifugation (www.sigma-zentrifugen.de) and NUVE OT012 steam sterilizer (www.nuve.com.tr) was used at sterilization for bacterial studies. Spectrophotometric measurements were carried out with SHIMADZU UV-1700 (www.pharmaspec.com) UV-Visible spectrometer. Fourier transform infrared spectroscopy (FT-IR) analyses were carried out on a Thermo-Scientific, Nicolet iS10-ATR spectrophotometer (www.thermoscientific.com) and samples were prepared in potassium bromide pellets. TGA 4000 Thermogravimetric Analyzer, Perkin Elmer (www.perkinelmer.com) was used for TGA analysis.

Synthesis of GO and graphene-Pt nanoparticles

GO was prepared by modifying the Hummers–Offeman method [19]. 1 g of graphite powder was added into 23 mL 98 % H_2SO_4 solution and stirred at room temperature for 24 h. After

that, 100 mg of $NaNO_3$ was added into the mixture and stirred for 30 min. Then 46 mL water was added to above mixture drop by drop. *Note:* This step should be executed with great care and by using safety goggles because it is highly exothermic. The water addition lasted for 25 min. Finally, 140 mL of water and 10 mL of 30 % H_2O_2 were added into the mixture to stop the reaction. The unexploited graphite in the resulting mixture was removed by centrifugation.

A 10 mg portion of GO powder was dispersed in 10 mL of water by sonication for 1 h, forming stable GO colloid [20, 21]. Then 20 mL of EG and 0.5 mL of 0.01 M H_2PtCl_6 were added to the solution and stirred for 30 min. Subsequently, the mixture was put in an oil bath and heated at 100 °C for 6 h with magnetic stirring. The graphene-Pt hybrid NPs were centrifuged to separate from the EG solution and washed with deionized water for five times. The resulting products were dried in a vacuum oven at 60 °C for 12 h [11]. Finally, the prepared graphene-Pt hybrid NPs dispersed to 10 mg mL^{1-} in water by ultrasonication and stored at 4 °C when not used [15].

Preparation of *G. oxydans* culture

The strain of *G. oxydans DSM 2343* was obtained from DSMZ (German Collection of Microorganisms and Cell Cultures, Braunschweig, Germany, www. dsmz.de). *G. oxydans* was maintained on the agar containing (g L^{-1}): D-glucose, 100; yeast extract, 10; calcium carbonate, 20; agar, 20 [22]. The cell biomass was prepared by aerobic cultivation at 28 °C on a rotary shaker in 250 mL flasks filled with 50 mL of media. The growth medium contained glucose, 0.5 % and yeast extract, 0.5 %. The culture, inoculated from the slant agar, was incubated for 17 h at 28 °C in a shaking incubator to reach the late exponential phase. The cell growth was followed spectrophotometrically via measuring optical density at 600 nm to obtain the same amount on the electrode surface [23]. Strain stocks were stored at −180 °C with 25 % (v v^{1-}) of glycerol at early phase. Then, for the electrochemical measurements, the cells from one of the cultivation flasks were collected by centrifugation (10 min, 4000×g), re-suspended in sterile 0.9 % NaCl solution and centrifuged again. After removal of washing solution completely from the cells, bacterial pellet was dissolved in required amount of pH 6.5 PB. These solutions were stored at −18 °C when not in use.

Preparation of electrodes

Plain microbial biosensor was prepared by mixing 80 % glassy carbon microparticles with 20 % mineral oil and 3.0 μL *G. oxydans* cell (5.08×10^{9} cell titer). Resulting paste was filled into 2 mm radius sized hole of Teflon body where copper wire was provided as electrical contact for the electrode. The *G.oxydans*/GCPE surface was polished on a paper. Also *G.oxydans*/GO/GCPE and G.oxydans/graphene-Pt hybrid NP/GCPE were obtained by addition of proper amounts of nanomaterials to the paste structure.

Sample application

Two types of glucose solutions were prepared at 1 and 2 μM concentrations. One solution was the synthetically prepared plasma sample that contained 140 mM NaCl, 4.5 mM KCl, 2.5 mM $CaCl_2$, 0.8 mM $MgCl_2$, 2.5 mM urea, 0.35 g dl^{-1} bovine serum albumin and 62 mg dl^{-1} immunoglobulin G in 10 mM 10 mL Tris–HCl solution [24]. This solution was well mixed and pH of the solution was adjusted to the 7.3 with 1.0 M HCl solution. Then, standard glucose solutions (at 1 or 2 μM concentrations) were prepared in this synthetic serum sample. The other glucose solutions were prepared just by using PB as solvent. After the cyclic voltammetric examination of developed biosensor, recovery values were calculated by comparison of obtained currents from synthetic serum and PB media.

Results and discussion

As mentioned at above sections, graphene-Pt hybrid NPs were prepared by reducing GO with EG-water mixture in the

Scheme 1 Reaction mechanism of glucose bioconversion [25]

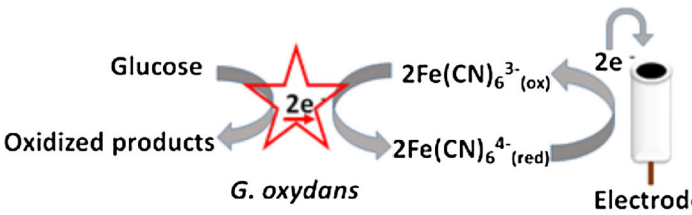

$$\text{Glucose} + \textit{G. Oxydase}_{(ox)} \rightarrow \text{Gluconic acid} + \textit{G. Oxydase}_{(red)}$$

$$\textit{G. Oxydase}_{(red)} + 2\,Fe(CN)_6^{3-}{}_{(ox)} \rightarrow \textit{G. Oxydase}_{(ox)} + 2\,Fe(CN)_6^{4-}{}_{(red)} + 2H^+$$

$$2\,Fe(CN)_6^{4-}{}_{(red)} \rightarrow 2\,Fe(CN)_6^{3-}{}_{(ox)} + 2e^-$$

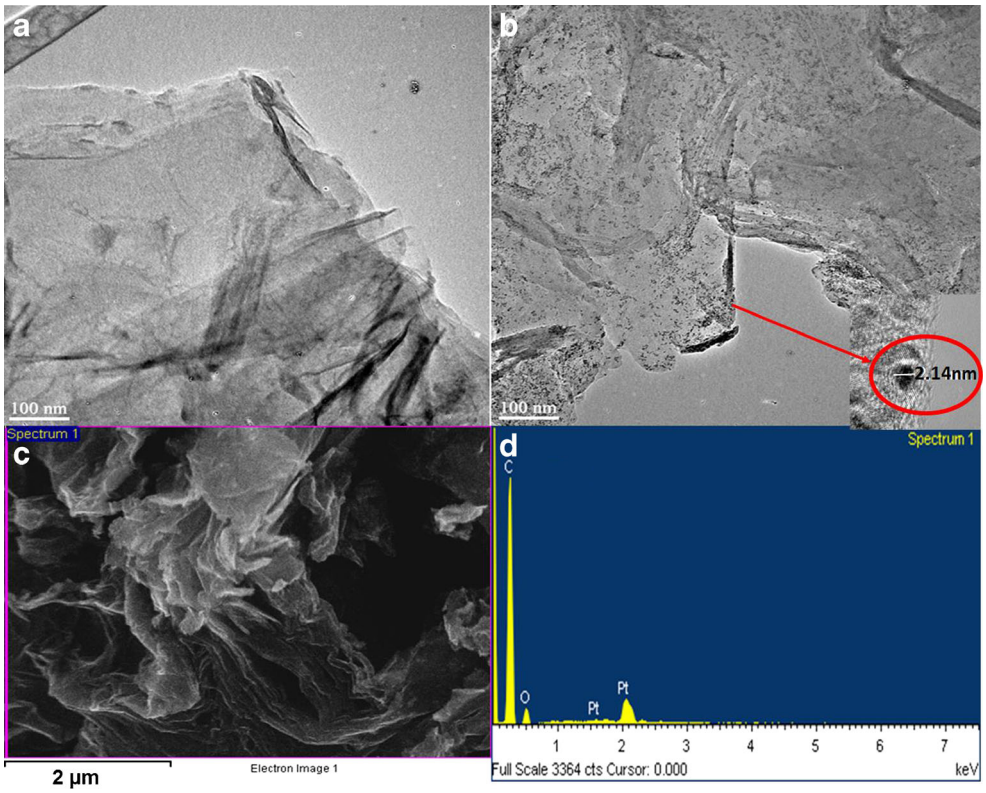

Fig. 1 TEM images of **a**: GO and **b**: graphene-Pt hybrid NP (inset: size of Pt nanoparticle=2.14 nm), **c**: SEM image of graphene-Pt hybrid NP, D: EDS of graphene-Pt hybrid NP

presence of Pt-salt. Among the three types of noble metals, Pt, Pd and Au, it was observed that Pt provides the most deoxygenation of GO sheets [11]. From the XPS results, Xu et al., proved that hydroxyl groups were also eliminated when Pt salts were used in the reduction procedure [11]. For this reason we decided to produce the same material and observe its effect in microbial biosensors.

After the production and optimization of GO and graphene-Pt hybrid NP amounts, these nanostructures combined with *G.Oxydans* modified GCPE electrode and as a result glucose biosensor was obtained. The redox mechanism involves the monitoring of oxidation of $Fe(CN)_6^{3-}$ to $Fe(CN)_6^{4-}$ as shown in the literature [25]. The mechanism implies that while glucose is converted into gluconic acid via GOx enzymes on the bacteria, GOx enzyme is reduced. Then, GOx (red) reduces $Fe(CN)_6^{3-}$ to $Fe(CN)_6^{4-}$ and in the last step $Fe(CN)_6^{4-}$ is oxidized to $Fe(CN)_6^{3-}$(Scheme 1). As a result, this mediation cycle produces a current, depends on the glucose concentration [25]. So after addition of glucose into the medium, current increase is expected due to the oxidation of $Fe(CN)_6^{4-}$ (Scheme 1) [25, 26]. As it is seen in Fig. 3 *G.oxydans*/GCPE biosensor is selective for glucose and shows expected increment whereas *G. Oxydans* free GCPE does not show any increase in the current response. As a result, the potential applied between −0.4 and 1.0 V range and the oxidation of $Fe(CN)_6^{4-}$ to $Fe(CN)_6^{3-}$ was recorded (Scheme 1) [25, 26].

Characterizations of synthesized nanostructures

TEM images of synthesized GO and graphene-Pt hybrid NP are given in Fig. 1a and b. Figure 1b inset shows the 20 times magnified TEM image of graphene-Pt hybrid NPs. As can be seen from the Figure, the size of one Pt nanoparticles on

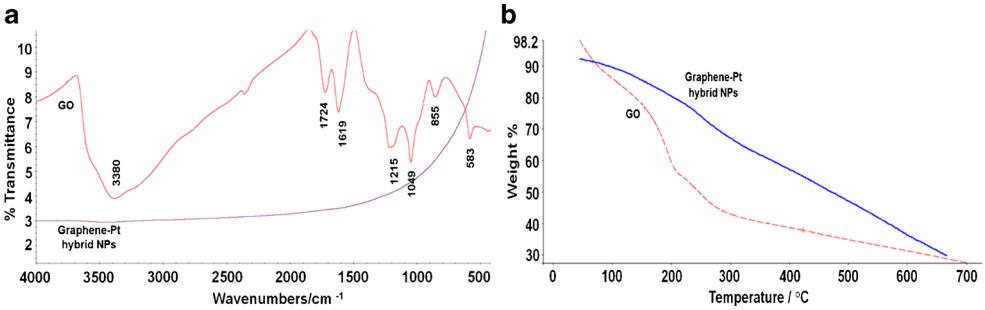

Fig. 2 **a** FT-IR characterizations of GO and graphene-Pt hybrid NP, **b** TGA characterizations of GO and graphene-Pt hybrid NP

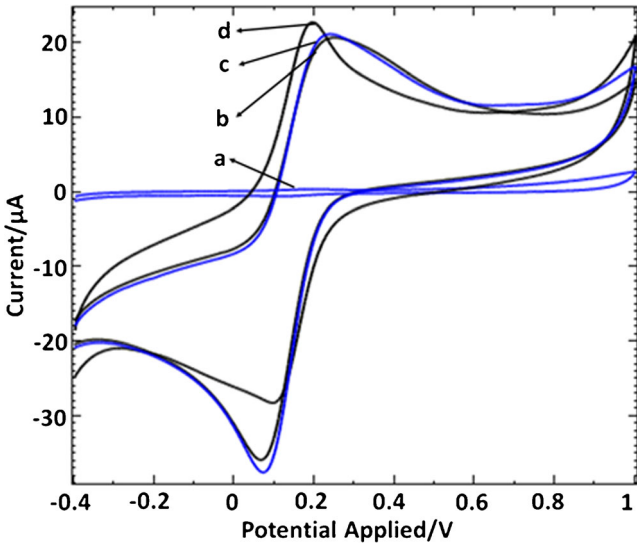

Fig 3 Cyclic voltammograms of **a**) *G. Oxydans* modified GCPE in 50 mM pH: 6.5 PB, **b**) *G. Oxydans* modified GCPE in 2 mM $K_3Fe(CN)_6$ including PB, **c**) *G. Oxydans* free GCPE in 20 mM glucose and 2 mM $K_3Fe(CN)_6$ including PB **d**) *G. Oxydans* modified GCPE in 20 mM glucose and 2 mM $K_3Fe(CN)_6$ including PB (at 100 mV s^{1-} scan rate)

graphene was measured as 2.14 nm. Also SEM image and EDS result of graphene-Pt hybrid NPs are given in Fig. 1c and d. As can be seen from Fig. 1a GO nanostructure is in a two dimensional sheet form. Also Pt nanoparticles are placed onto graphene sheets homogenously (Fig. 1b). Figure 1c and d show that atomic dispersion percentages of hybrid NPs were 87.92 %, 11.22 %, 0.86 % and mass percentages of these elements were 75.29, 12.80 and 11.91 % for C, O and Pt respectively. So these results prove that graphene-Pt hybrid NP was prepared successfully.

Also FT-IR and TGA characterizations of GO and graphene-Pt hybrid NP were given in Fig. 2a and b. FT-IR spectrum of GO shows the absorption bands corresponding to C=O carbonyl stretching at 1724 cm^{-1}, C-OH stretching at 1215 cm^{-1}, and C-O stretching at 1049 cm^{-1} [27, 28]. Also the peak at 1619 cm^{-1} corresponds to the remaining sp^2 character of C=C [29]. After reduction by EG, most of the functional groups are removed. The peak absorption band at around 3380 cm^{-1} which is attributed to –OH stretching vibrations and also the peak absorption band at around 1635 cm^{-1} which belongs to carboxyl groups are definitely decreases demonstrating the effective deoxygenation of GO via EG and Pt salts [11, 30, 31].

TGA was preformed from 50 to 700 °C at a heating rate of 5 °C /min under nitrogen flow and results are presented in Fig 2b. TGA curve of GO shows that GO was thermally unstable and starts to lose mass upon heating below 100 °C due to the adsorbed water. There is a significant drop in mass around 215 °C which is assigned to the evolution of CO and CO_2 from GO caused by the destruction of oxygenated functional groups [11]. On the other hand, as can clearly be seen from the Figure, the weight loss at around 200 °C in the graphene-Pt hybrid NP is much lower than GO. This is clearly caused by the reduction of oxygenated functional groups due to the presence of Pt [11].

Electrochemical characterizations of the biosensors

Performance of *G.oxydans*/GCPE biosensor was tested before optimization studies to observe if *G. oxydans* cells works properly. Thus cyclic voltammograms of *G.oxydans*/GCPE

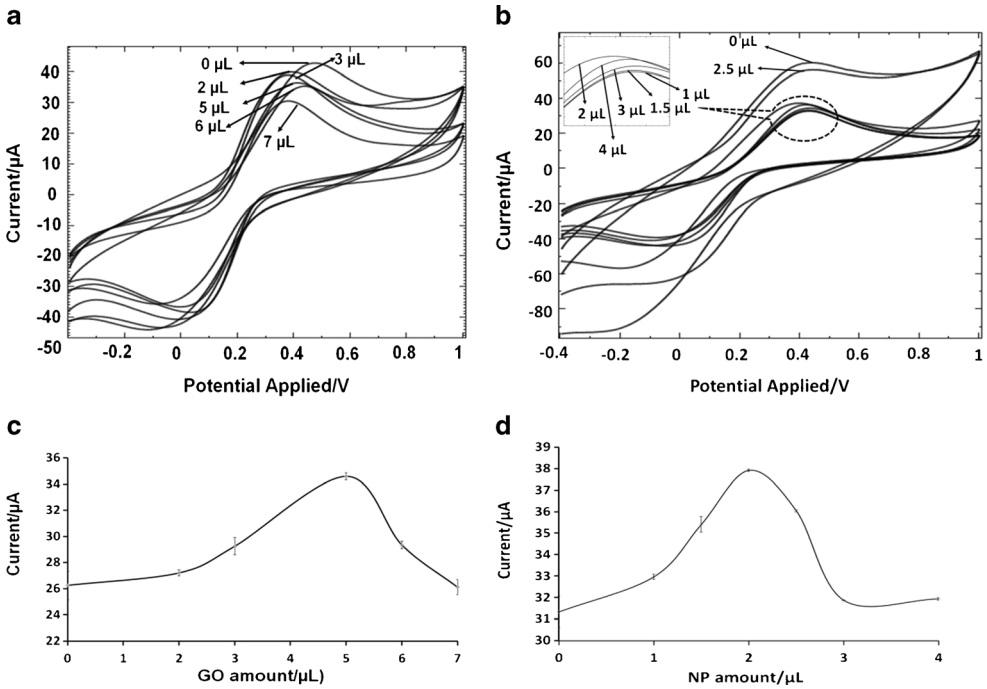

Fig. 4 Cyclic voltammograms of **a**) GO amount, **b**) graphene-Pt hybrid NP amount optimizations and corresponding optimization graphics of **c**) GO amount, D) graphene-Pt hybrid NP amount for microbial biosensors.

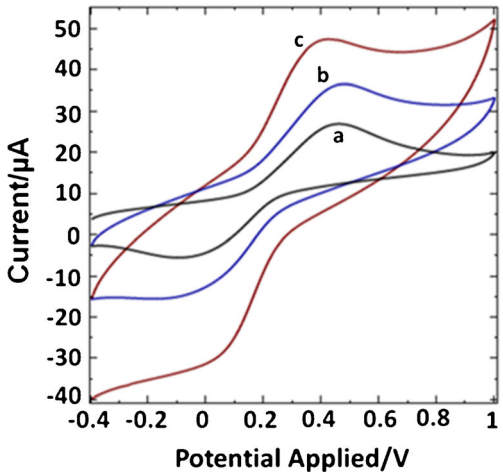

Fig. 5 Cyclic voltammograms of a) *G.oxydans*/GCPE, b) *G.oxydans*/GO /GCPE c) *G.oxydans*/graphene-Pt NP/GCPE microbial biosensors.

biosensor were recorded in PB, in 2 mM $K_3Fe(CN)_6$ containing PB and 20 mM glucose and in 2 mM $K_3Fe(CN)_6$ containing PB respectively. Also, the response of *G. Oxydans* free GCPE was examined in PB including 20 mM glucose and 2 mM $K_3Fe(CN)_6$. Then all of the voltammograms are compared in Fig. 3. As can clearly be seen from the Figure, when glucose was added to the medium, increase in current together with shift at peak potential has been observed. This demonstrates that *G.Oxydans* works properly and uses glucose as substrate according to the mechanism that was explained at the beginning of the results and discussion part.

After obtaining the expected electrochemical signal, the experimental conditions were optimized by using cyclic voltammetry. In this concept, amount of *G. oxydans* onto the biosensor response was examined (Fig. S1). 1.0, 2.0, 3.0, 4.0 and 5.0 μL of cells were added into the composite structure of GCPE and as a result, 3.0 μL was found as optimum cell amount. Subsequently pH (Fig. S2A), working temperature (Fig. S2B) and incubation time (Fig. S2C) parameters were also optimized by using plain (without any nanocomposite) *G.oxydans*/GCPE microbial biosensor. The electrode was renewed for every measurement. Since the best results were obtained at pH 6.5, 25 °C and 10 s further studies were conducted by utilizing these values. Detailed information was given in Electronic Supplementary Material.

Comparison of nanostructure amounts

Optimum GO and graphene-Pt hybrid NP amounts were examined under the optimum working conditions. In this concept 3.0 μL of *G. oxydans* cell was used in the electrode preparation, then cyclic voltammograms were recorded after 10 s incubation time at 25 °C in 2.0 mM $K_3Fe(CN)_6$ and 20 mM glucose containing 10 mL 50 mM (pH 6.5) PB between −0.4 and 1.0 V potential range with 100 mV s^{1-} scan rate. In order to define optimum nanostructure amount, *G.oxydans*/ GO /GCPE microbial biosensors were prepared with addition of 0, 2, 3, 5, 6 and 7 μL GO suspensions (at 2 μg μL^{1-} concentration) into the paste structure. As can be seen from the Fig. 4A, up to 5 μL of GO addition, current

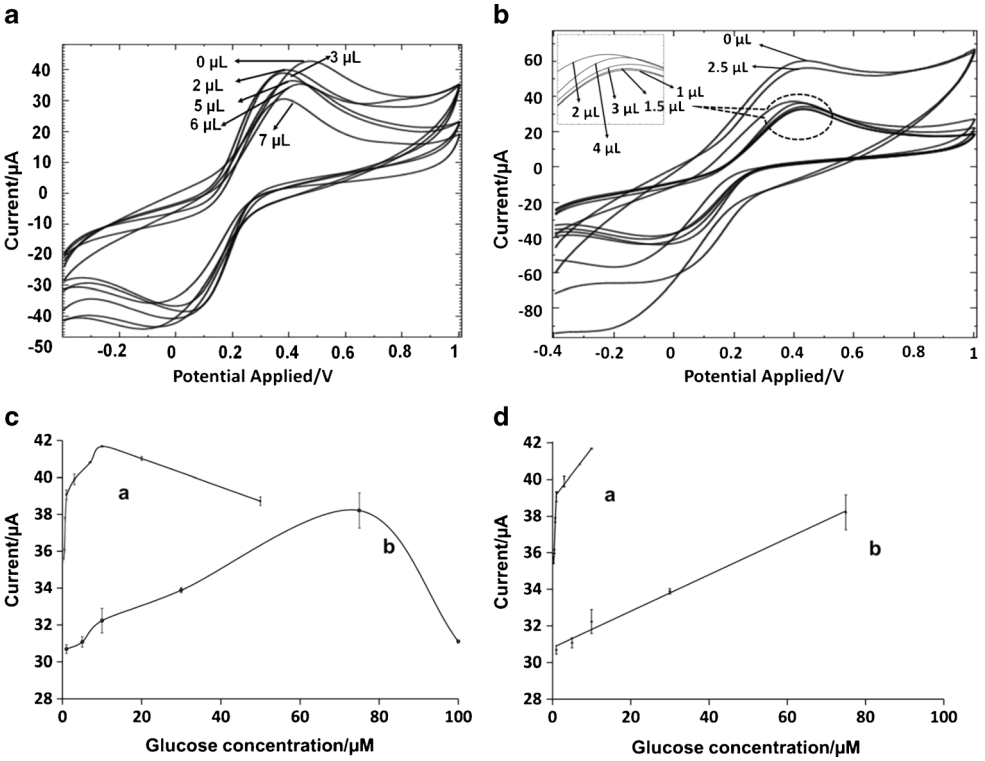

Fig. 6 **A** Cyclic voltammograms of *G.oxydans*/graphene-Pt hybrid NP/GCPE, **B** Cyclic voltammograms of *G.oxydans*/GO/GCPE microbial biosensor, **C** Analytical ranges of a) *G.oxydans*/graphene-Pt hybrid NP/GCPE, b) *G.oxydans*/GO/GCPE microbial biosensor, **D** Linear ranges of a) *G.oxydans*/graphene-Pt hybrid NP/GCPE, b) *G.oxydans*/GO/GCPE microbial biosensor

response increases but above this value biosensor response decreases sharply. Also for the graphene-Pt hybrid NP amount optimizations, the same steps were followed with *G.oxydans*/graphene-Pt NP/GCPE microbial biosensors, thus 0, 1, 1.5, 2, 2.5, 3, and 4 μL nanocomposite suspensions (at 2 μg μL^{1-} concentrations) were introduced into the electrode structure. For this study, maximum current value was obtained at 2 μL (Fig. 4B). Since the best current values were obtained with 5 μL GO and 2 μL graphene-Pt hybrid NP suspensions, these amounts were used for further experiments.

Effects of nanostructure addition into microbial biosensor

Figure 5 exhibits the comparison of the effects of GO and graphene-Pt hybrid NP onto *G.oxydans* biosensor's response. Measurements were recorded under optimum conditions as stated above. Current differences between nanostructure modified and plain biosensors show that graphene-Pt hybrid NP modification was more effective at the response enhancement of the developed microbial glucose biosensor (Fig. 5) (current values for *G.oxydans*/graphene-Pt NP/GCPE; 36.90 μA, for *G.oxydans*/ GO /GCPE; 31.04 μA, for *G.oxydans*/GCPE microbial biosensor; 27.80 μA). We believe that this is due to the introduction of Pt into graphene structure.

Analytical characteristics

After determination of GO and graphene-Pt hybrid NP optimum amounts, linear ranges of microbial biosensors were examined for varying glucose concentrations for each modification respectively. *G.oxydans*/ GO /GCPE showed a linear range 1–75 μM with equation of $y=100.10x+30.78$ ($R^2=0.990$) and analytical range of 1–100 μM (Fig. 6Cb-Db). *G.oxydans*/graphene-Pt hybrid NP/GCPE showed two linear ranges as 0.3-1 and 1–10 μM and analytical range was 1–50 μM for this electrode (Fig. 6Ca-Da). Also linear range calibration equations of *G.oxydans*/graphene-Pt hybrid NP/GCPE were obtained as $y=5261.50x+33.84$ and $y=279.34x+38.89$ (R^2 values were 0.965 and 0.989 respectively). Measurements were recorded under optimum conditions in 2.0 mM $K_3Fe(CN)_6$ containing 50 mM pH: 6.5 PB between −0.4 and 1.0 V potential range with 100 mV s^{1-} scan rate. RSD value of *G.oxydans*/GO/GCPE was calculated as 0.14 % (n=3) while for *G.oxydans*/graphene-Pt hybrid NP/GCPE biosensor the value is 0.21 % (n=3). On the other hand, *G.oxydans*/graphene-Pt hybrid NP/GCPE has better LOD (3 s/m) and LOQ (10 s/m) values compared to *G.oxydans*/GO/GCPE (LOD: 0.015±0.002 μM and LOQ: 0.049±0.002 μM for *G.oxydans*/graphene-Pt hybrid NP/GCPE and LOD 1.062±0.030 μM, and LOQ 3.541±0.030 μM for *G.oxydans*/GO/GCPE respectively (n=3)).

Analytical characteristics of the developed electrochemical microbial biosensors were also compared with previous *G. Oxydans* based glucose biosensor studies in terms of linear ranges and LOD values (Table 1). According to the Table, developed method has the smallest LOD value and linear range in μM levels cofirming the sensitivity of G.oxydans/graphene-Pt hybrid NP/GCPE and G.oxydans/GO/GCPE microbial biosensors.

Sample application

G.oxydans/graphene-Pt NP/GCPE microbial biosensor was applied to the glucose determination in the synthetic plasma sample solution. The current values were measured for three times for each solution and the average current values and recovery values were given in Table 2. As it is described in the experimental section, glucose solutions were prepared

Table 2 Current responses of *G.oxydans*/graphene-Pt hybrid NP/GCPE microbial biosensor for 1 and 2 μM glucose standard solutions prepared in synthetic serum solution and PB.

	Glucose in PB	Glucose in synthetic serum	Recovery value(%)
Current values/μA (for 1 μM)	37.7	38.4	101.8
Current values/μA (for 2 μM)	34.3	35.8	104.4

Table 1 Comparison of analytical characteristics of G.oxydans/graphene-Pt hybrid NP/GCPE and G.oxydans/GO/GCPE microbial biosensors with previous *G. Oxydans* based glucose biosensor studies.

Electrode type	Applied method	Linear range	LOD	Reference
G.Oxydans/thiol-functionalized Fc/AuNP/Gold electrode	Amperometry	0.5 to 10 mM	0.17 mM	[32]
G.Oxydans/PANI/PDDS/Ag/Graphite electrode	Cyclic voltammetry	0.1–3.0 mM	–	[33]
G. oxydans/HKCN/graphite electrode	Flow injection analysis	0.1–7.5 mM	–	[34]
G. oxydans/CHIT–Fc/GCE	Flow injection analysis	1.5 to 25.0 mM	0.797 mM	[35]
G.oxydans/GO/GCPE	Cyclic voltammetry	1–75 μM	1.062±0.030 μM	Present study
G.oxydans/graphene-Pt hybrid NP/GCPE	Cyclic voltammetry	0.3–1 and 1–10 μM (two linear ranges)	0.015±0.002 μM	Present study

both in synthetic plasma solutions and in PB individually at the concentrations of 1 and 2 μM. Then results were compared and recovery values were calculated (Table 2). From the results it is obvious that developed biosensor can be applied to complicated sample solution without observing any matrix effect.

Selectivity

Selectivity of the *G.oxydans*/graphene-Pt hybrid NP/GCPE microbial biosensor was examined with glucose in the presence of fructose and galactose as possible interferent agents. Measurements were carried out in the same concentration and increasing concentrations like 5, 7, 10 and 100 folds of interferents (Table S1). Electrode was renewed before all measurements. From the results it can be concluded that developed biosensor can be used in the presence up to 100 fold amounts of these sugars with current difference of 13.60 %. We also examined the selectivity of the *G.oxydans*/graphene-Pt hybrid NP/GCPE microbial biosensor in the presence of L-ascorbic acid and dopamine in the same amount and increasing concentrations like 2, 5, 10, 50 and 100 folds of interferents (Table S2). Results showed that G.oxydans/graphene-Pt NP/GCPE microbial biosensor can work up to 100 folds of these interferents with 12.07 % current difference.

Storage stability

Storage stability of microbial biosensor was examined for different periods of time. *G.oxydans*/graphene-Pt hybrid NP/GCPE microbial biosensor was stored at +4 °C in pH 6.5 PB for 1 day, 1 week and 1 month. After these periods, the recovery values were calculated as 99.6, 102 and 97.5 % respectively. These values show that developed *G.oxydans* biosensor is very stable and can be used for long period of time.

Conclusions

Unique properties of graphene nanostructures were employed in this study as usage of GO and graphene-Pt hybrid NP in microbial biosensor where *G.oxydans* was used as whole cell in the GCPE. GO and graphene-Pt hybrid NP addition into biosensor structure resulted with higher current responses. Actually both of graphene nanostructure enhanced the sensitivity of whole cell biosensor but as we looked to analytical characteristic values, graphene-Pt hybrid NP addition made the best contribution (LOD values are 0.015±0.002 μM and 1.062±0.03 μM for graphene-Pt hybrid NP and GO). Also for sample application, acceptable recovery values were obtained demonstrating the applicability of the developed biosensor. Considering obtained current values for selectivity and stability studies of *G.oxydans*/graphene-Pt NP/GCPE microbial biosensor, it can be concluded that developed system is selective and stable enough. So further studies will continue in our lab for the adaptation of this favorable system to *G.oxydans* based microbial biofuel cells.

Acknowledgments The grant from Muğla Sıtkı Koçman University BAP Project number 13 / 17 is greatly acknowledged.

References

1. Anik Ü, Çevik S, Pumera M (2010) Effect of nitric acid "washing" procedure on electrochemical behavior of carbon nanotubes and glassy carbon μ-particles. Nanoscale Res Lett 5:846–852
2. Çevik S, Anik Ü (2010) Banana tissue-nanoparticle/nanotube based glassy carbon paste electrode biosensors for catechol detection. Sens Lett 8:667–671
3. Apetrei I, Apetrei C (2015) The biocomposite screen-printed biosensor based on immobilization of tyrosinase onto the carboxyl functionalised carbon nanotube for assaying tyramine in fish products. J Food Eng 149:1–8
4. Pumera M (2009) Electrochemistry of graphene: new horizons for sensing and energy storage. Chem Rec 9:211–223
5. Wang Y, Li Y, Tang L, Lu J, Li J (2009) Application of graphene-modified electrode for selective detection of dopamine. Electrochem Commun 11:889–892
6. Bo Y, Yang H, Hu Y, Yao T, Huang S (2011) A novel electrochemical DNA biosensor based on graphene and polyaniline nanowires. Electrochim Acta 56:2676–2681
7. Shan C, Yang H, Song J, Han D, Ivaska A, Niu L (2009) Direct electrochemistry of glucose oxidase and biosensing for glucose based on graphene. Anal Chem 81:2378–2382
8. Zhou M, Zhai Y, Dong S (2009) Electrochemical sensing and biosensing platform based on chemically reduced graphene oxide. Anal Chem 81:5603–5613
9. Khim Chng EL, Chua CK, Pumera M (2014) Graphene oxide nanoribbons exhibit significantly greater toxicity than graphene oxide nanoplatelets. Nanoscale 6(18):10792–10797
10. Georgakilas V, Gournisb D, Tzitziosa V, Pasquato L, Guldie DM, Prato M (2007) Decorating carbon nanotubes with metal or semiconductor nanoparticles. J Mater Chem 26:2679–2694
11. Xu C, Wang X, Zhu J (2008) Graphene-metal particle nanocomposites. J Phys Chem C 112:19841–19845
12. Li D, Kaner RB (2008) Graphene-based materials. Science 320: 1170–1171
13. Xing YC (2004) Synthesis and electrochemical characterization of uniformly-dispersed high loading Pt nanoparticles on sonochemically-treated carbon nanotubes. J Phys Chem B 108: 19255–19259
14. Novoselov KS, Geim AK, Morozov SV, Jiang D, Katsnelson MI, Grigorieva IV, Dubonos SV, Firsov AA (2005) Two-dimensional gas of massless Dirac fermions in graphene. Nature 438:197–200
15. Sultan SC, Anik Ü (2014) Gr–Pt hybrid NP modified GCPE as label and indicator free electrochemical genosensor platform. Talanta 129:523–528
16. Tepeli Y, Anik U (2015) Comparison of performances of bioanodes modified with graphene oxide and graphene-platinum hybrid nanoparticles. Electrochem Commun. doi:10.1016/j.elecom.2015.05.002
17. Alferov SV, Tomashevskaya LG, Ponamoreva ON, Bogdanovskaya VA, Reshetilov AN (2006) Biofuel cell anode based on the gluconobacter oxydans bacteria cells and 2,6-dichlorophenolindophenol as an electron transport mediator. Elektrokhimiya 42:456–457

18. Tkac J, Svitel J, Vostiar I, Navratil M, Gemeiner P (2009) Membrane-bound dehydrogenases from gluconobacter sp.: interfacial electrochemistry and direct bioelectrocatalysis. Bioelectrochemistry 76:53–62
19. Hummers WSJ, Offeman R (1958) Preparation of graphitic oxide. J Am Chem Soc 80:1339–1339
20. Li D, Müller MB, Gilje S, Kaner RB, Wallace GG (2008) Processable aqueous dispersions of graphene nanosheets. Nat Nanotechnol 3:101–105
21. Stankovich S, Dikin DA, Dommett GH, Kohlhaas KM, Zimney EJ, Stach EA, Piner RD, Nguyen ST, Ruoff RS (2006) Systematic post-assembly modification of graphene oxide paper with primary alkylamines. Nature 442:282–286
22. Vostiar I, Ferapontova EE, Gorton L (2004) Electrical wiring of viable Gluconobacter oxydans cells with flexible osmium-redox polyelectrolyte. Electrochem Commun 6:621–626
23. Gatgens C, Degner U, Bringer-Meyer S, Hermann U (2007) Biotransformation of glycerol to dihydroxyacetone by recombinant Gluconobacter oxydans DSM 2343. Appl Microbiol Biotechnol 76:553–559
24. Coldur F, Andac M, Isildak I (2010) Flow-injection potentiometric applications of solid state Li^{+} selective electrode in biological and pharmaceutical samples. J Solid State Electrochem 14:2241–2249
25. Wang J (2001) Glucose biosensors: 40 years of advances and challenges. Electroanalysis 13:983–988
26. Tkac J, Vostiar I, Gorton L, Gemeiner P, Sturdık E (2003) Improved selectivity of microbial biosensor using membrane coating. Biosens Bioelectron 18:1125–1134
27. Matsuo Y, Miyabe T, Fukutsuka T, Sugie Y (2007) Preparation and characterization of alkylamine-intercalated graphite oxides. Carbon 45:1005–1012
28. Kovtyukhova NI, Ollivier PJ, Martin BR, Mallouk TE, Chizhik SA, Buzaneva EV, Gorchinskiy AD (1999) Layer-by-layer assembly of ultrathin composite films from micron-sized graphite oxide sheets and polycations. Chem Mater 11:771–778
29. Herrera-Alonso M, Abdala AA, McAllister MJ, Aksay IA, Prud'homme RK (2007) Intercalation and stitching of graphite oxide with diaminoalkanes. Langmuir 23:10644–10649
30. Li D, Müller MB, Gilje S, Kaner RB, Wallace GG (2007) Processable aqueous dispersions of graphene nanosheets. Nat Nanotechnol 3:101–105
31. Zhang L, Li N, Jiu H, Qi G, Huang Y (2015) ZnO-reduced graphene oxide nanocomposites as efficient photocatalysts for photocatalytic reduction of CO2. Ceram Int 41:6256–6262
32. Yildirim N, Odaci Demirkol D, Timur S (2015) Modified gold surfaces with gold nanoparticles and 6-(ferrocenyl)hexanethiol: design of a mediated microbial sensor. Electroanalysis 27:52–57
33. Sharifirad M, Kiani F, Koohyar F (2014) Design of a microbial sensor using a conducting polymer of polyaniline/poly 4,4'-diaminodiphenyl sulphone-silver nanocomposite films on a carbon paste electrode. Mater Technol 48:209–214
34. Guler E, Soyleyici HC, Odaci Demirkol D, Ak M, Timur S (2014) A novel functional conducting polymer as an immobilization platform. Mater Sci Eng C 40:148–156
35. Yılmaz Ö, Odacı Demirkol D, Gülcemal S, Kılınc A, Timur S, Cetinkaya B (2012) Chitosan–ferrocene film as a platform for flow injection analysis applications of glucose oxidase and Gluconobacter oxydans biosensors. Colloids Surf B: Biointerfaces 100:62–68